

Learning to Manipulate Anything: Revealing Data Scaling Laws in Bounding-Box Guided Policies

Yihao Wu¹, Jinming Ma², Junbo Tan^{1†}, Yanzhao Yu¹,
Shoujie Li¹, Mingliang Zhou², Diyun Xiang², Xueqian Wang^{1†}

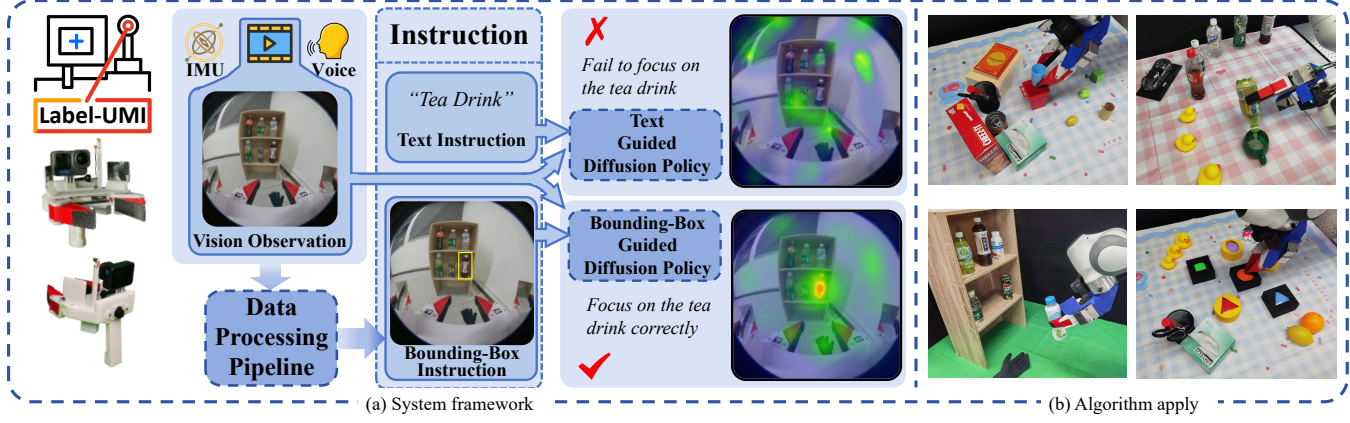


Fig. 1: Overview of framework. (a) The Label-UMI device collects multimodal demonstration data including IMU, visual observations, and voice commands. This data is processed through an automated pipeline that utilizes the segmentation laser point cues to generate bounding box labels overlaid on the images. When provided as input to the Bounding-Box Guided Diffusion Policy, these visual bounding box instructions lead to more robust and target-concentrated policy behavior compared to text instruction conditioning, as evidenced by sharper attention maps. (b) Demonstration of the Bounding-Box Guided Diffusion Policy (BBox-DP).

Abstract—Diffusion-based policies show limited generalization in semantic manipulation, posing a key obstacle to the deployment of real-world robots. This limitation arises because relying solely on text instructions is inadequate to direct the policy’s attention toward the target object in complex and dynamic environments. To solve this problem, we propose leveraging bounding-box instruction to directly specify target object, and further investigate whether data scaling laws exist in semantic manipulation tasks. Specifically, we design a handheld segmentation device with an automated annotation pipeline, Label-UMI, which enables the efficient collection of demonstration data with semantic labels. We further propose a semantic-motion-decoupled framework that integrates object detection and bounding-box guided diffusion policy to improve generalization and adaptability in semantic manipulation. Throughout extensive real-world experiments on large-scale datasets, we validate the effectiveness of the approach, and reveal a power-law relationship between generalization performance and the number of bounding-box objects. Finally, we summarize an effective data collection strategy for semantic manipulation, which can achieve 85% success rates across four tasks on both seen and unseen objects. All datasets and code will be released to the community.

I. INTRODUCTION

Data scaling laws [1] have significantly accelerated the development of natural language processing and computer

vision, as evidenced by the success of large language models [2] (e.g., GPT) and vision-language models [3] (VLMs). Recently, the robotics community has started to explore a similar question: whether similar scaling laws exist in robotic semantic manipulation. Unfortunately, research in this area remains scarce. A fundamental obstacle is that policies relying solely on text instructions, as commonly studied, often fail to achieve robust semantic manipulation themselves. This failure occurs because, under identical observations, multiple manipulable objects or feasible actions may coexist. It is difficult for such a policy to focus on task objectives from text instruction alone [4] as illustrated in Fig.1(a), especially in cluttered and noisy environments where semantic ambiguity is further amplified. Without a policy that can reliably perform the task, conducting a systematic study on how its performance scales with data becomes infeasible.

To obtain reliable semantic manipulation policies, one category of methods encodes text instructions into features fused with visual inputs via FiLM or cross-attention, improving semantic alignment for policy networks. Models like Diff-Control [5], OCTO [6], and RDT-1B [7] follow this paradigm, yet they rely heavily on large-scale language-annotated demonstration datasets—often requiring millions of image–text–action triplets for robust performance [8], which introduces substantial scalability constraints. Another category employs pre-trained LLMs to interpret language commands directly, leveraging their broad semantic knowledge to enhance instruction understanding. Methods such as OpenVLA [9], OpenVLA-OFT [10], and ChatVLA [11] incorporate models like Llama for improved linguistic ground-

*Work done during the internship at Xiaomi Robotics Lab.

¹Center for Intelligent Control and Telescience, Tsinghua Shenzhen International Graduate School, Shenzhen, China.

²Beijing Xiaomi Robot Technology Co., Ltd 602, 6th Floor, Building 5, No. 15 10th Kechuang Street, Beijing Economic-Technological Development Area, Beijing, China, 100176

†Corresponding author: {tjblql, wang.xq}@sz.tsinghua.edu.cn

ing and expert-activated reasoning. Despite strengthened language capability, these systems often face practical issues such as high computational cost, limited real-time performance, and increased complexity. A third category employs fine-grained visual guidance—such as 2D trajectory sketches or 3D keypoints—to direct policy attention. Techniques like Rt-Trajectory [12] and HAMSTER [13] overlay motion sketches, while KITE [14] grounds instructions in part-level 3D keypoints. These approaches, however, often depend on specific camera perspectives, dense 3D sensing, or detailed annotations, which can limit their applicability in scalable, egocentric, or minimally-instrumented settings.

In this paper, we propose a semantic-motion decoupled architecture for robotic semantic manipulation, featuring a novel collaborative reasoning mechanism between object detection models and diffusion policy models. As shown in Fig. 4, our framework first extracts the target object through semantic text and transforms it into a bounding-box visual representation—a design choice motivated by the bounding box’s optimal balance between annotation efficiency and providing sufficient spatial guidance, distinct from methods that rely on more intricate geometric representations.

Building on this, our framework can alleviate the generalization challenges of semantic manipulation by explicitly presenting the target object as a “bounding-box visual instruction”, which is more directly interpretable by the policy than textual instruction. This insight aligns with principles observed in biological learning [15]: infants primarily acquire knowledge and learn to manipulate objects through visual exploration rather than linguistic cues, illustrating the effectiveness of visually grounded task representations.

By combining these bounding-box visual instructions with a diffusion-based policy, our semantic-motion decoupled framework effectively transfers the generalization in semantic manipulation to the object detection module, such as YOLO [16] or more advanced vision-language models. In this design, the diffusion-based policy only needs to learn to follow the bounding-box visual instructions; in other words, manipulate any object specified by a bounding box. Furthermore, we systematically investigate the existence of data scaling laws in semantic manipulation tasks. Through extensive real-world experiments on large-scale datasets, we demonstrate the effectiveness of our framework and reveal a power-law relationship between generalization performance and the number of bounding-box objects, highlighting how increasing the diversity of object annotations systematically improves policy generalization in semantic manipulation tasks. Motivated by this finding, we propose a dedicated data collection strategy for semantic manipulation and empirically validate its effectiveness.

Overall, our contributions can be summarized as follows:

- **Handheld semantic annotation device.** We design Label-UMI, a lightweight handheld segmentation device that extends the UMI system. The Label-UMI enables efficient demonstration data collection in the wild, and it provides accurate semantic annotations labels through segmentation points.

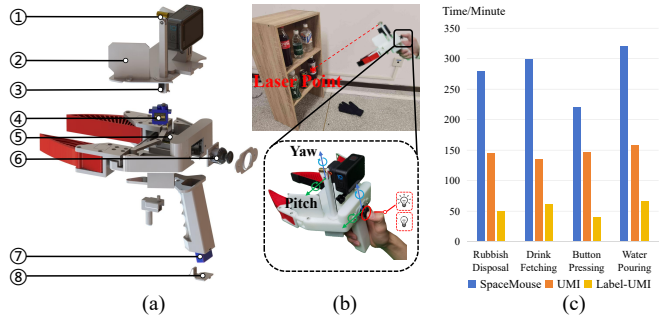


Fig. 2: (a) Structure of Label-UMI. Composition of the Label-UMI Device Components: ①Laster, ②Mirror, ③Mini servo motor, ④SG90 servo motor, ⑤ESP32 microcontroller, ⑥PS2 joystick controller, ⑦Battery, ⑧U-shaped bayonet mount. (b) The Label-UMI Data Collection Operating Procedure. (c) Comparison of the time required to collect and annotate 100 data samples across different devices.

- **Bounding-Box Guided Diffusion Policy.** We propose the Bounding-Box Guided Diffusion Policy (BBox-DP), a semantic-motion decoupled control framework that can integrate any object detection modules with a diffusion-based policy. This framework explicitly leverages bounding boxes as “visual instructions”, thereby transferring generalization capability to the detection module and enhancing semantic manipulation performance. Extensive experiments demonstrate that our method achieves strong performance in diverse semantic manipulation tasks and generalizes to unseen objects.
- **Data scaling law for semantic manipulation.** Through large-scale experiments, we reveal a power-law relationship between generalization performance and the number of annotated bounding-box objects. Building on this insight, we propose a data collection strategy tailored to semantic manipulation. With this strategy, the policy achieves around 85% success rates across four real-world tasks for both seen and unseen objects, validating the scalability and practicality of our approach.

II. RELATED WORK

A. Data Collection and Diffusion Policy for Robotic Manipulation

Robotic data collection is a fundamental step for training manipulation policies. Early approaches relied on teleoperation [17], where human operators controlled robots to execute tasks and gather demonstrations. This has been achieved through techniques such as virtual reality (VR) teleoperation [18], [19] and leader-follower kinematic setups [20]. However, these methods are often limited by high costs and constrained operational scenarios, making large-scale collection in the wild impractical. More recently, handheld portable devices [21], [22] have emerged, enabling platform-independent data collection in diverse environments. Yet, these systems typically lack continuous annotation of key object information, such as shape, position, or masks, which are crucial for effective semantic manipulation.

In parallel, diffusion models have gained attention in robotic manipulation for their strong generative and generalization capabilities. For example, Chi et al. [23] applied

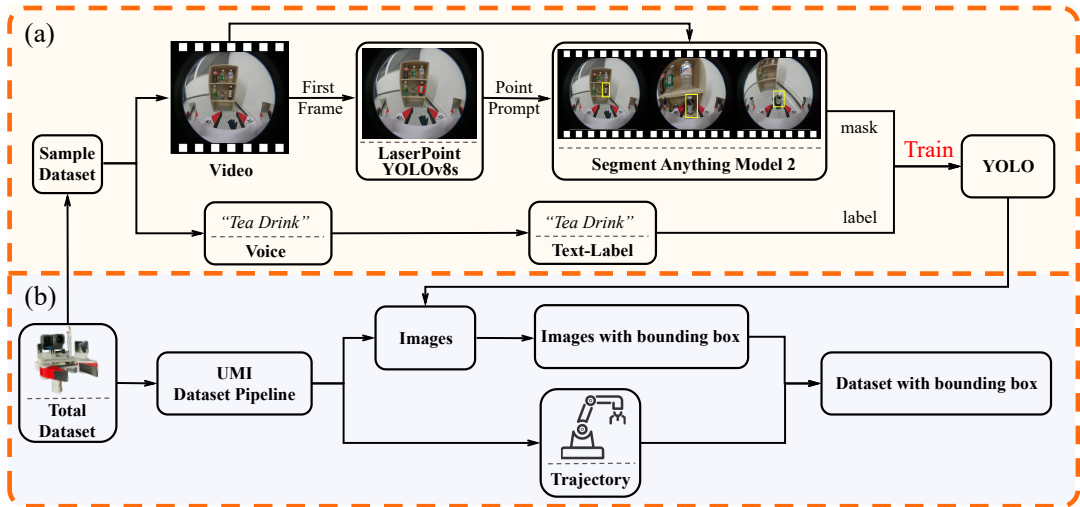


Fig. 3: Overview of Data Acquisition pipeline. (a) YOLO model acquisition process. We randomly sample a subset from the total dataset. The first video frame and the LaserPoint-YOLOv8s model are used to locate the laser point serving as a prompt. This prompt, together with the full video, is fed into the SAM2 to segment the object and generate a bounding box for each video frame. A YOLO model is then trained to detect the object using the text label and the image annotated with the bounding box. (b) Full dataset (w/ BBox) acquisition process. We leverage the UMI data pipeline to extract trajectory and image information. The trained YOLO model is then applied to automatically annotate images with bounding boxes, resulting in a full dataset with bounding box labels.

diffusion models to visuomotor learning to improve long-horizon task performance, while Black et al. [24] explored zero-shot manipulation by leveraging pre-trained diffusion policies for adaptable task execution. Despite these advances, existing methods struggle to handle semantic grasping and manipulation tasks, where object-level perception and generalization remain major challenges. Our work addresses this gap by integrating bounding-box guided object information into diffusion-based policies, improving both generalization and adaptability in semantic manipulation scenarios.

B. Application of Bounding Boxes in Robot Manipulation

Bounding boxes play a crucial role in vision-based robotic grasping [25], particularly in object localization [26], pose estimation [27], and grasp planning [28]. In object detection, bounding boxes precisely locate target objects by defining rectangular regions within image or point cloud data. This functionality not only provides the foundation for object localization but also establishes a key prerequisite for subsequent tasks such as pose estimation and grasp planning. Bounding boxes enhance complex systems; in Im2Flow2Act [29], they refine grasping by initializing keypoint sampling and filtering, and in ManiBox [28], they form a low-dimensional state representation for streamlined predictions. Recently, bounding boxes have also been adopted as foundational representations for high-level reasoning. For example, ECoT [30] employs bounding boxes as intermediate reasoning tokens to ground language instructions, while energy-based scene rearrangement models [31] optimize configurations of bounding boxes to satisfy compositional language constraints. In contrast to these prior uses, our work focuses on bounding boxes as scalable visual instructions for policy learning, and systematically studies the empirical scaling laws between bounding-box object diversity and policy generalization.

Most methods use YOLO or its variants [32] for bounding box prediction, while others design networks [33] like ResNet-101 with RPN for ROI generation and detection. However, acquiring labeled data is very time-consuming. Consequently, some methods [29] [28] have begun to employ zero-shot semantic detection models like Grounding DINO. However, these approaches tend to perform poorly in open-ended environments and exhibit lower detection accuracy for objects described with rich adjectives. In this paper, we propose a novel data acquisition and annotation method, which enhances efficiency while maintaining accuracy.

III. METHOD

In this section, we first introduce the hardware design and data processing pipeline for batch data collection. We then present an improved diffusion policy leveraging bounding box representations. Finally, we provide a formal formulation of the data scaling laws and describe our rigorous evaluation protocol.

A. Integrated Data Acquisition and Processing Pipeline

The core research question addressed by our framework is how to efficiently obtain a labeled dataset in which target objects are annotated with bounding boxes—critical for object localization and grasp planning. However, existing robotic manipulation datasets do not provide enough environments and objects for a single task to meet our requirements. Given the proven effectiveness of data collected by the UMI device [21] in training diffusion policies, we designed the Lable-UMI with an ergonomic form factor inspired by UMI.

This design ensures accurate baseline reproduction and enhances experimental comparability. As illustrated in Fig. 2(a), the Label-UMI comprises a compact gimbal with a laser emitter and a PS2 joystick controller. The laser provides precise target object positioning and segmentation point cues. Users control the laser's pitch and yaw via the joystick and

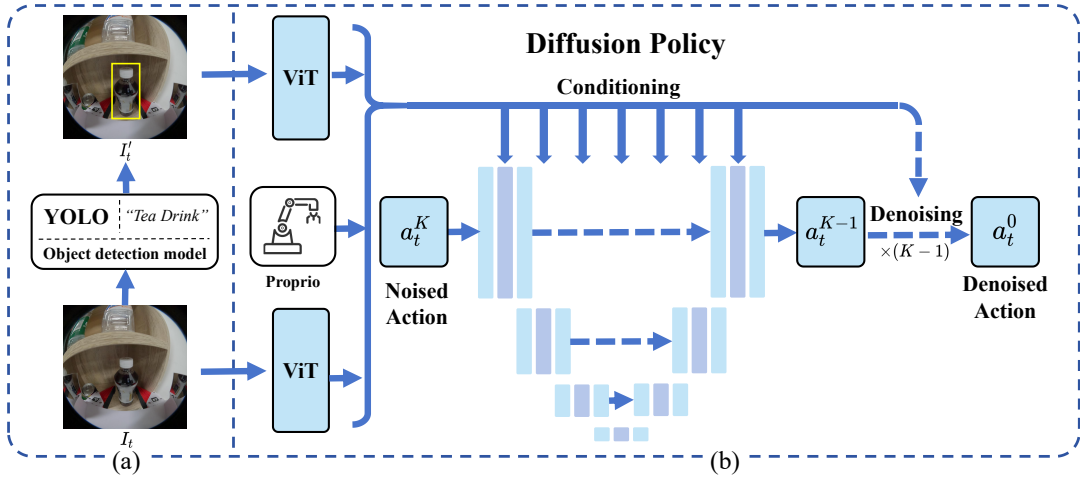


Fig. 4: Overview of the BBox-DP. (a) Semantic detection part. The raw image and the image overlaid with bounding boxes (generated by YOLO) are encoded separately using a ViT. (b) Main policy part. The resulting visual features are then combined with the robot’s proprioceptive state to form a unified conditioning signal. This multimodal condition guides a U-Net-based diffusion model to iteratively denoise the action sequence, ultimately yielding the refined, denoised action output.

toggle the laser on and off using the joystick button (Fig. 2(b)). The ergonomic design allows intuitive operation: the thumb controls the joystick while the index finger triggers data acquisition, similar to a game controller.

We improved upon the UMI design by replacing the rack-and-pinion mechanism with a multi-link system, reducing weight and freeing internal space for microcontrollers, servos, and other electronics. The power unit is integrated into the handle with a U-shaped bayonet mount for easy battery replacement, enhancing portability, field usability, and user experience. To collect data with segmentation point markers, the user first aligns the laser with the target object using the joystick, starts video recording, verbally states the object name into the GoPro microphone, and then executes the task. This procedure ensures synchronized data and annotation capture.

The data processing pipeline (Fig. 3) automates the extraction of bounding box labels and trajectory data. After collection, audio is transcribed to obtain object labels, while the first video frame is processed by LaserPoint-YOLOv8s—a YOLOv8s model fine-tuned for laser point detection—to locate the laser dot. Its center coordinates serve as a point prompt input along with the video into Segment Anything Model 2 (SAM2), which generates per-frame object masks. Minimum bounding boxes are derived from these masks. This automated pipeline yields high-precision bounding box annotations for each object in every frame, used to train a real-time YOLO detection model. The approach offers three key advantages:

- **High labeling efficiency:** The entire labeling process is fully automated via script files, thereby eliminating the need for manual label assignment (as shown in Fig. 2(c)).
- **Fast inference speed:** Compared with zero-shot object detection models like Ground DINO, our model achieves faster inference due to its fewer parameters, making it ideal for real-time robotic tasks.
- **High labeling accuracy:** Our pipeline utilizes SAM2’s

high accuracy and robustness to achieve fast and precise object segmentation in complex scenes, showcasing strong performance and wide applicability.

Motion trajectories are processed using ORB-SLAM3, following the UMI framework [21], and are not detailed here. After dataset construction, we employ it to train two key components: a *Bounding-Box Detection Module* and a *Bounding-Box Guided Diffusion Policy*.

B. Bounding-Box Detection Module

Detection models such as DINOv2 provide accurate and robust bounding boxes, but their high computational cost limits real-time deployment in robotic systems. Furthermore, such zero-shot models often struggle with abstract or out-of-distribution objects in some situations, which are difficult to detect via text prompts. They also exhibit limited discriminative capability for fine-grained categories, such as distinguishing different beverage brands, despite reliably recognizing general object categories like “drink.”

To balance accuracy and efficiency, we adopt a YOLO-based detector trained with data generated by our automated pipeline. This approach achieves real-time performance with high accuracy while maintaining flexibility. By decoupling semantic detection from the main policy into a modular visual instruction interface, the detection module can be seamlessly replaced in the future with more advanced models that offer improved speed or precision, without affecting the overall inference performance of the system.

To clearly illustrate how this module is utilized across different stages, we distinguish between training and inference. During training, the bounding boxes are generated by our *Data Acquisition and Processing Pipeline*, which leverages a laser to accurately localize and annotate the operational objects. During inference, we employ a YOLO model trained via our Data Acquisition Pipeline, considering task-specific characteristics. Leveraging our decoupled architecture, the target’s bounding box can be specified through modalities like eye-gaze recognition, natural language instructions via

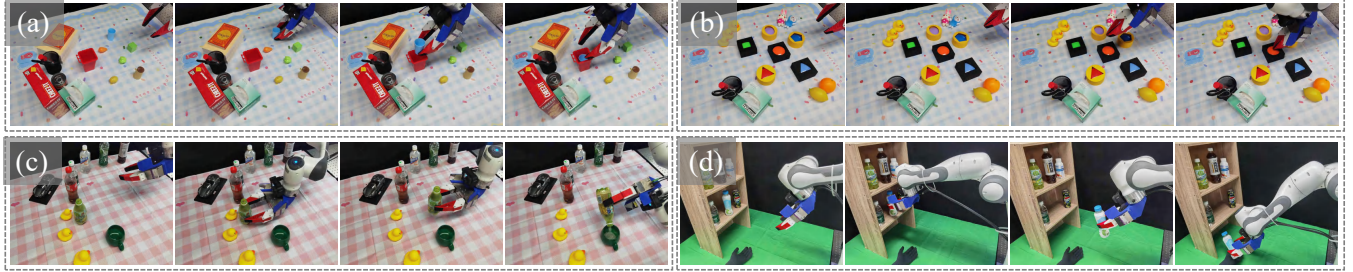


Fig. 5: Real-robot experiments on four semantic manipulation tasks: (a) **Rubbish Disposal** – the robot identifies a specified piece of rubbish, grasps it, and discards it into a trash bin; (b) **Button Pressing** – the robot selects and presses a designated button among multiple visually similar distractors; (c) **Water Pouring** – the robot grasps a target container and pours its contents accurately into a cup; (d) **Drink Fetching** – the robot locates a prompted drink from a multi-layer shelf, grasps it, and delivers it to a human.

an LLM, or external detection models, as long as detection performance meets task requirements.

C. Bounding-Box Guided Diffusion Policy

After training the detection module, we now turn to the core of our framework—the policy model. We introduce an end-to-end imitation learning framework, termed **BBox-DP**, which extends diffusion policies to model multi-modal action distributions conditioned on visual observations enriched with bounding box annotations, as illustrated in Fig.4.

Specifically, at time step t , the semantic instruction L is first processed by a object detection model, which highlights the target object by generating a bounding box on the input image I_t , thereby producing an augmented image I'_t . Both the original image I_t and the annotated image I'_t are subsequently fed into a pre-trained Vision Transformer (ViT) for feature extraction. Here, I_t represents the raw RGB image of the physical environment, which contains object contour information essential for determining the grasping posture, whereas I'_t explicitly represents the relative spatial location of the target object.

The extracted features explicitly supply positional cues of the target object, which directly guide the diffusion policy to generate action trajectories toward the object over K denoising steps. We utilize a CNN-based U-Net ε_θ as the noise prediction network and adopt DDIM [34] to reduce inference latency, thereby enabling real-time control. The policy is trained using the loss function defined in Eq. (1). This design not only improves the interpretability of the visual representations but also improves the generalization of the model to novel, previously unseen objects.

$$\mathcal{L} = \text{MSE}(\varepsilon^k, \varepsilon_\theta(\mathbf{O}_t, \mathbf{a}_t^0 + \varepsilon^k, k)) \quad (1)$$

where ε^k is the noise added at diffusion step k , \mathbf{O}_t includes the raw image I_t , the bounding-box annotated image I'_t , and proprioceptive state information *proprio*, and k denotes the current denoising iteration step.

IV. FORMALIZATION OF DATA SCALING WITH BOUNDING BOXES

Building on prior work in data scaling for robotic imitation learning [35], where generalization performance S is modeled as a function of environments (M), object instances (N), and demonstrations per object–environment pair (K),

each object O_i in environment E_j is associated with K demonstrations $(D_{ij}^1, \dots, D_{ij}^K)$ while environments include arbitrary distractors from other categories. In this paper, we extend this framework to investigate how increasing the number of bounding-box objects improves generalization across diverse object categories.

Unlike earlier settings restricted to N objects from a single category, we introduce N' arbitrary object classes $(H_1, H_2, \dots, H_{N'})$ without constraining distractors, and annotate each demonstration with bounding boxes for these objects. The policy is then evaluated on unseen environments and objects using the score S (described later). Our investigation focuses on twofold: (1) to characterize how S scales with the number of bounding-box objects N' and demonstrations per object class K ; and (2) to identify efficient data collection strategies for achieving strong generalization.

To ensure reliable evaluation, we adopt three measures. First, policies are tested exclusively on unseen environments and unseen objects to assess generalization. Second, we employed human-assigned stage-wise scores (typically 2–3 stages per task; see Section V), producing a normalized score that captures nuanced behavior beyond binary success/failure. Finally, to minimize evaluator bias, multiple policies trained on varying dataset sizes are compared simultaneously. For fair comparison, each rollout was randomly selected from these policies while ensuring identical initial conditions for the object and robot.

V. EXPERIMENTS

In this section, we first evaluate the effectiveness of our bounding-box-guided algorithm compared with other semantics-guided baselines (Sec. V-B). Next, we investigate how increasing the diversity of objects annotated with bounding boxes influences generalization performance, from which we derive power-law data scaling trends (Sec. V-C). Based on these findings, we propose an efficient data collection strategy that enhances the generalization capability of policies centered on semantic objectives (Sec. V-D). Finally, we validate the proposed data collection strategy on additional tasks to demonstrate its cross-task data efficiency (Sec. V-E).

A. Overview of Experiments

To thoroughly evaluate the effectiveness of our method, we designed four real-world robotic manipulation tasks,

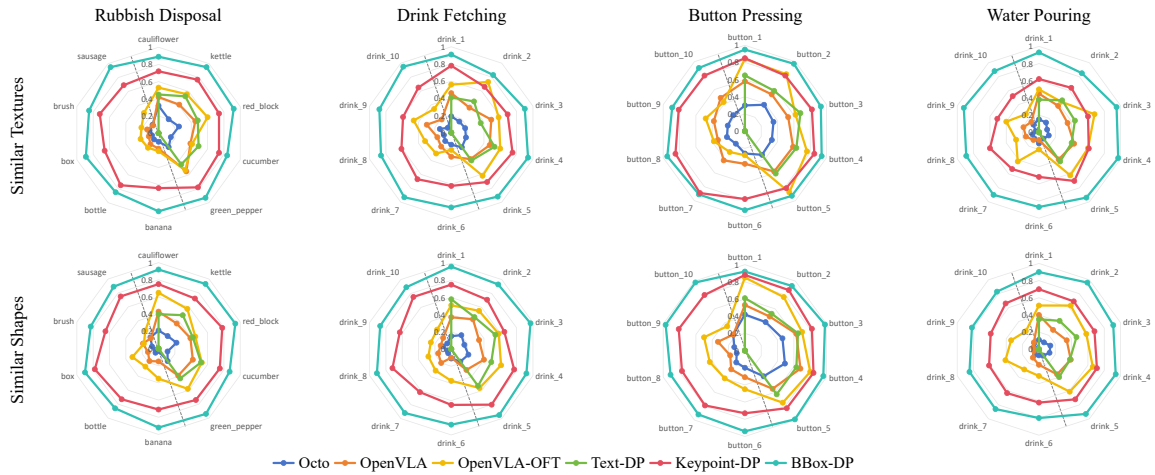


Fig. 6: The performance score for each operational object. In each radar chart, objects to the left of the dashed line represent the test set, while those to the right belong to the training set. Since beverage brands and custom-designed buttons are difficult to differentiate textually, we represent them using codes; the full mapping between codes and objects is provided in the supplementary video due to space constraints.

TABLE I: Quantitative Results. We evaluate the success rates of Octo, OpenVLA, OpenVLA-OFT, Text-DP, and our proposed BBox-DP across four real-world tasks. Sim. Tex. denotes distractor objects with similar textures, while Sim. Shape denotes distractor objects with similar shapes.

Policy	Rubbish Disposal		Drink Fetching		Button Pressing		Water Pouring	
	Sim. Tex.	Sim. Shape	Sim. Tex.	Sim. Shape	Sim. Tex.	Sim. Shape	Sim. Tex.	Sim. Shape
Octo	0.16	0.13	0.14	0.13	0.28	0.30	0.11	0.09
OpenVLA	0.29	0.28	0.33	0.25	0.48	0.43	0.27	0.23
OpenVLA-OFT	0.37	0.42	0.46	0.43	0.58	0.60	0.44	0.46
Text-DP	0.48	0.45	0.43	0.52	0.63	0.61	0.42	0.40
Keypoint-DP	0.72	0.75	0.66	0.70	0.85	0.81	0.57	0.66
BBox-DP(ours)	0.90	0.91	0.89	0.92	0.93	0.95	0.91	0.88

as shown in Fig. 5: Rubbish Disposal, Drink Fetching, Button Pressing, and Water Pouring. All tasks are conducted in cluttered environments containing multiple homogeneous distractor objects, requiring the robot to accurately identify and manipulate the target object based on the given prompt. For dataset construction, each task was configured with $M = 4$ environments and $N' = 16$ object classes. For each object class, 25 demonstrations were collected in environments, producing 100 valid demonstrations per object. Consequently, each task contains a total of 1600 valid demonstrations.

These four tasks comprehensively evaluate the policy’s ability to perform multi-step manipulation and instruction following. To enable fine-grained evaluation, each task is divided into multiple stages. Specifically, Rubbish Disposal, Drink Fetching, and Water Pouring are each divided into three stages: (i) whether the robot approaches the correct target, (ii) whether it successfully grasps the target, and (iii) whether it completes the final action (discarding, handing over, or pouring). Button Pressing is divided into two stages: (i) whether the robot approaches the designated button and (ii) whether it presses it successfully. The overall performance is quantified using Eq. (2):

$$S = \eta \cdot \frac{1}{n} \sum_{m=1}^n S_m + \lambda \cdot \text{clip}\left(1 - \frac{t - t_{\min}}{t_{\max} - t_{\min}}, 0, 1\right) \quad (2)$$

where the first term is the average stage score where $S_m \in \{0, 1\}$ indicates success at stage m over n stages; and the

second term measures time efficiency based on the actual completion time t within thresholds t_{\min} and t_{\max} ; η, λ are weighting coefficients with $\eta + \lambda = 1$.

B. Comparison with Semantics-Guided Baselines

Our experiments aim to evaluate the necessity of visual object guidance for semantic manipulation. We compare a range of policy architectures employing varying forms of semantic conditioning. To more comprehensively assess visual representation choices, we include a point-based guidance alternative as an additional baseline. The baselines considered are as follows:

- **Octo:** A transformer-based foundation model [6] pre-trained on large-scale robot data for action generation.
- **OpenVLA:** A 7B parameter VLA [9] model based on Llama-2 and CLIP [36], serving as a strong full-fine-tuning baseline.
- **OpenVLA-OFT:** A parameter-efficient variant of OpenVLA [10] using Orthogonal Fine-Tuning to improve generalization while reducing parameters.
- **Text-DP:** A text-conditioned diffusion policy [23] fusing text and image features via FiLM, without relying on explicit bounding-box guidance.
- **Keypoints-DP:** A variant of our framework that uses 2D keypoints (extracted from SAM2 mask centroids) as visual guidance, inspired by object-centric conditioning methods [37].

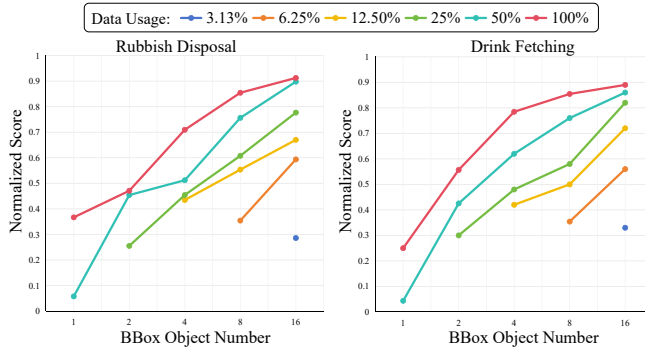


Fig. 7: Generalization across Bounding-Box Object Number.

For each baseline, five operational objects were sampled from the training set and another five from the test set. Each policy was tested over 10 randomized trials per object, with results averaged and quantified using Eq. (2). Since Text-DP was not pre-trained on internet-scale data, it was evaluated only on five training-set objects. To systematically assess robustness under different distraction settings, we categorized distractor objects into two types: (1) objects with similar shapes but different textures compared to the target, and (2) objects with similar textures but distinct shapes.

The experimental results are summarized in Table I, with the performance score for each operational object detailed in Fig. 6. Our proposed Bounding-Box Guided Diffusion Policy consistently outperforms all baselines across tasks. Notably, compared to both Text-DP (no visual guidance) and Keypoints-DP (point-based guidance), our method shows substantial improvement, highlighting the advantage of bounding boxes as a richer and more robust visual instruction format. A Welch’s t-test was conducted on the success rates of each evaluation, yielding p-values of $p = 3.36310^{-7}$ for Rubbish Disposal, $p = 9.73610^{-4}$ for Drink Fetching, $p = 4.05710^{-4}$ for Button Pressing, and $p = 7.52310^{-3}$ for Water Pouring. On this basis, we reject the null hypothesis that the diffusion policy with box guidance does not improve success rates.

Furthermore, compared to pre-trained open-source models such as Octo, OpenVLA and OpenVLA-OFT, our method also outperforms them, demonstrating the effectiveness of explicitly leveraging bounding boxes as “visual instructions” to guide the policy.

C. Scaling Laws for Bounding Box Generalization

We first investigate two manipulation tasks: Rubbish Disposal and Drink Fetching, using the same dataset described in Section V-B, which contains 1600 demonstrations per task. To study how the number of bounding boxes objects affects policy generalization and how policy performance varies with the number of demonstrations, we define a triple $(m, n)_j$. Here, $m = 0, 1, 2, 3, 4$ represents the number of object with bounding boxes 2^m sampled from the pool of 16, $n = 0, -1, -2, -3, -4, -5$ denotes the fraction of demonstrations per object as 2^n , and j is the repetition index. When $m < 4$, we perform five independent random samplings ($j \in [1, 5]$), while for $m = 4$, only one sampling

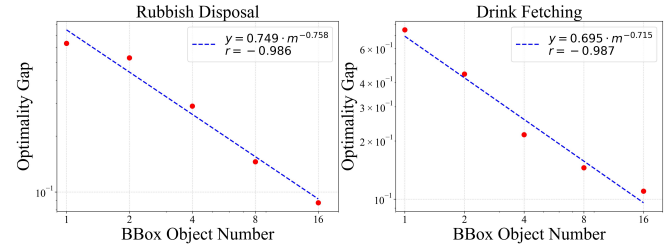


Fig. 8: Power-law relationship.

is performed ($j = 1$). Policies are trained for each valid $(m, n)_j$ combination with more than 50 total demonstrations, resulting in 76 trained policies. Each policy is evaluated on 16 unseen objects in an unseen environment, with 5 trials per object, yielding an average performance score $(m, n)_j$ over 80 trials. The final score for each (m, n) configuration is computed by averaging across all repetitions j .

As shown in Fig. 7, we summarize the experimental results for both tasks, revealing two key findings: (1) The policy’s generalization performance consistently improves as the number of bounding-box objects increases, across all demonstration fractions. (2) Increasing the number of bounding-box objects reduces the number of demonstrations needed per object. For example, in Rubbish Disposal, using 4 bounding-box objects produces a noticeable performance gap between 50% and 100% demonstration fractions, whereas this gap nearly disappears when 16 objects are used.

Then, we examine whether these results follow a power-law scaling behavior, commonly observed in other machine learning domains. A power-law relationship between two variables Y and X is defined as $Y = \beta \cdot X^\alpha$, which can be linearized via logarithmic transformation: $\log(Y) = \alpha \log(X) + \log(\beta)$. In our setting, Y corresponds to the optimality gap (i.e., $1 - \text{NormalizedScore}$), and X represents the number of bounding-box objects. Using data from the experiments with 100% demonstration fraction, we fit a linear model to the log-transformed values, as illustrated in Fig. 8. The results indicate that: the policy’s generalization to new objects, new environments, or both scales approximately as a power law with the number of bounding-box objects, as evidenced by the correlation coefficient r in Fig. 8.

D. Efficient Data Collection for Generalizable Policies

In this section, we present a data collection strategy derived from the data scaling laws, aiming to address a practical question: *Given a manipulation task, how should one select the number of object classes with bounding box annotations (N') and the number of demonstrations per object (K) to maximize generalization without excessive data collection effort?* We illustrate this using the Rubbish Disposal and Drink Fetching tasks.

The first question is how to optimally select both the number of objects with bounding box annotations and the number of demonstrations per object. As revealed in Section V-C, once the performance score reaches 50, increasing the diversity of annotated objects yields greater improvements than simply increasing demonstrations. This effect is especially evident when $K = 50$, where performance grows most

TABLE II: Success rate across all tasks.

Task	Rubbish Disposal	Drink Fetching	Button Pressing	Water Pouring
Score	89.78	86.45	91.21	87.36
Success Rate	90.45%	87.43%	92.26%	86.79%

rapidly. Notably, when the number of objects reaches 16, the model’s performance approaches approximately 85%.

Based on these findings, we recommend the following strategy: *whenever possible, prioritize collecting a diverse set of objects (around 16 in total), while providing approximately 50 demonstrations per object*. This strategy offers an effective balance between performance gains and resource expenditure. Only when object diversity can no longer be increased further due to resource constraints, and maximal performance is essential, should one consider increasing the number of demonstrations per object.

The second question is which specific objects should be chosen for labeling, in order to optimize the policy’s generalization performance. In our earlier experiments, for each (m, n) combination with $m < 4$, we independently sampled five distinct sets of objects from the total of 16 object classes, yielding five distinct object combinations $(m, n)_j$. Evaluation of the corresponding policies revealed that performance scores vary considerably even when m and n are fixed; rather, the score strongly correlates with the shape variation of the object within the set. This effect is especially pronounced during the final approach stage of tasks, when the robotic arm is close to the target and preparing to grasp.

To further examine the role of shape variation, we set $m = 3$ and $n = 0$ (8 objects, full demonstrations per object), and generated 20 random subsets. After training and evaluating 20 corresponding policies, we found that generalization performance depends on both the uniformity of object counts across shape groups and the proportion of distinct shape groups. While the precise mechanism of this relationship leave to future work, we distill an empirical guideline for data collection: *for tasks involving significant shape variation among objects (e.g., Rubbish Disposal), training with highly shape-diverse objects significantly improves policy performance; in contrast, for tasks with limited shape variation (e.g., Drink Fetching), policy performance is less sensitive to shape diversity*.

E. Cross-Task Validation of Data Efficiency

To verify the general applicability of our data collection strategy, we applied it to two additional tasks: Button Pressing and Water Pouring. Data collection followed the efficient strategy derived from Section V-D. As indicated in Table II, the trained policies achieve success rates of around 85% across all four tasks, including both the previously studied tasks and the two newly introduced ones.

VI. CONCLUSIONS

In this work, we proposed a bounding-box guided policy framework that integrates the Label-UMI data collection device and the BBox-DP policy, which leverages visual

object cues (bounding-box) to enhance generalization in semantic manipulation. Moreover, we revealed a power-law relationship between performance and the number of annotated objects, leading to an object-diversity-first strategy for efficient dataset design. Extensive real-world experiments show that our method maintains over 85% success across diverse tasks, even with challenging texture- and shape-similar distractors. Overall, this work offers a scalable solution for semantic manipulation and highlights promising directions for data-efficient robot learning. As future work, we will investigate how the object shapes within the dataset affect policy performance.

REFERENCES

- [1] J. Kaplan, S. McCandlish, T. Henighan, T. B. Brown, B. Chess, R. Child, S. Gray, A. Radford, J. Wu, and D. Amodei, “Scaling laws for neural language models,” *arXiv preprint arXiv:2001.08361*, 2020.
- [2] J. Achiam, S. Adler, S. Agarwal, L. Ahmad, I. Akkaya, F. L. Aleman, D. Almeida, J. Altenschmidt, S. Altman, S. Anadkat, *et al.*, “Gpt-4 technical report,” *arXiv preprint arXiv:2303.08774*, 2023.
- [3] D. Zhu, J. Chen, X. Shen, X. Li, and M. Elhoseiny, “Minigpt-4: Enhancing vision-language understanding with advanced large language models,” *arXiv preprint arXiv:2304.10592*, 2023.
- [4] L. Zhuoling, R. Liangliang, Y. Jinrong, Z. Yong, *et al.*, “Vip: Vision instructed pre-training for robotic manipulation,” *arXiv preprint arXiv:2410.07169*, 2024.
- [5] X. Liu, Y. Zhou, F. Weigend, S. Sonawani, S. Ikemoto, and H. B. Amor, “Diff-control: A stateful diffusion-based policy for imitation learning,” in *2024 IEEE/RSJ International Conference on Intelligent Robots and Systems*. IEEE, 2024, pp. 7453–7460.
- [6] O. M. Team, D. Ghosh, H. Walke, K. Pertsch, K. Black, O. Mees, S. Dasari, J. Hejna, T. Kreiman, C. Xu, *et al.*, “Octo: An open-source generalist robot policy,” *arXiv preprint arXiv:2405.12213*, 2024.
- [7] S. Liu, L. Wu, B. Li, H. Tan, H. Chen, Z. Wang, K. Xu, H. Su, and J. Zhu, “Rdt-1b: a diffusion foundation model for bimanual manipulation,” *arXiv preprint arXiv:2410.07864*, 2024.
- [8] H. Liu, C. Li, Q. Wu, and Y. J. Lee, “Visual instruction tuning,” *Advances in neural information processing systems*, vol. 36, pp. 34 892–34 916, 2023.
- [9] M. J. Kim, K. Pertsch, S. Karamcheti, T. Xiao, A. Balakrishna, S. Nair, R. Rafailov, E. P. Foster, P. R. Sanketi, Q. Vuong, *et al.*, “Openvla: An open-source vision-language-action model,” in *Conference on Robot Learning*. PMLR, 2025, pp. 2679–2713.
- [10] M. J. Kim, C. Finn, and P. Liang, “Fine-tuning vision-language-action models: Optimizing speed and success,” *arXiv preprint arXiv:2502.19645*, 2025.
- [11] Z. Zhou, Y. Zhu, M. Zhu, J. Wen, N. Liu, Z. Xu, W. Meng, R. Cheng, Y. Peng, C. Shen, *et al.*, “Chatvla: Unified multimodal understanding and robot control with vision-language-action model,” *arXiv preprint arXiv:2502.14420*, 2025.
- [12] J. Gu, S. Kirmani, P. Wohlhart, Y. Lu, M. G. Arenas, K. Rao, W. Yu, C. Fu, K. Gopalakrishnan, Z. Xu, *et al.*, “Rt-trajectory: Robotic task generalization via hindsight trajectory sketches,” *International Conference on Learning Representations 2024*, 2023.
- [13] Y. Li, Y. Deng, J. Zhang, J. Jang, M. Memmel, R. Yu, C. R. Garrett, F. Ramos, D. Fox, A. Li, *et al.*, “Hamster: Hierarchical action models for open-world robot manipulation,” *International Conference on Learning Representations 2025*, 2025.
- [14] P. Sundaresan, S. Belkhale, D. Sadigh, and J. Bohg, “Kite: Keypoint-conditioned policies for semantic manipulation,” *The Conference on Robot Learning 2023*, 2023.
- [15] Z. Li, L. Ren, J. Yang, Y. Zhao, X. Wu, Z. Xu, X. Bai, and H. Zhao, “Vip: Vision instructed pre-training for robotic manipulation,” *arXiv preprint arXiv:2410.07169*, 2024.
- [16] R. Varghese and M. Sambath, “Yolov8: A novel object detection algorithm with enhanced performance and robustness,” in *2024 International conference on advances in data engineering and intelligent computing systems (ADICS)*. IEEE, 2024, pp. 1–6.

- [17] A. Mandlekar, Y. Zhu, A. Garg, J. Booher, M. Spero, A. Tung, J. Gao, J. Emmons, A. Gupta, E. Orbay, *et al.*, “Roboturk: A crowdsourcing platform for robotic skill learning through imitation,” in *Conference on Robot Learning*. PMLR, 2018, pp. 879–893.
- [18] X. Cheng, J. Li, S. Yang, G. Yang, and X. Wang, “Open-television: Teleoperation with immersive active visual feedback,” *arXiv preprint arXiv:2407.01512*, 2024.
- [19] T. Zhang, Z. McCarthy, O. Jow, D. Lee, X. Chen, K. Goldberg, and P. Abbeel, “Deep imitation learning for complex manipulation tasks from virtual reality teleoperation,” in *2018 IEEE international conference on robotics and automation*. Ieee, 2018, pp. 5628–5635.
- [20] T. Z. Zhao, V. Kumar, S. Levine, and C. Finn, “Learning fine-grained bimanual manipulation with low-cost hardware,” *arXiv preprint arXiv:2304.13705*, 2023.
- [21] C. Chi, Z. Xu, C. Pan, E. Cousineau, B. Burchfiel, S. Feng, R. Tedrake, and S. Song, “Universal manipulation interface: In-the-wild robot teaching without in-the-wild robots,” *arXiv preprint arXiv:2402.10329*, 2024.
- [22] H. Ha, Y. Gao, Z. Fu, J. Tan, and S. Song, “Umi on legs: Making manipulation policies mobile with manipulation-centric whole-body controllers,” *arXiv preprint arXiv:2407.10353*, 2024.
- [23] C. Chi, Z. Xu, S. Feng, E. Cousineau, Y. Du, B. Burchfiel, R. Tedrake, and S. Song, “Diffusion policy: Visuomotor policy learning via action diffusion,” *The International Journal of Robotics Research*, p. 02783649241273668, 2023.
- [24] K. Black, M. Nakamoto, P. Atreya, H. Walke, C. Finn, A. Kumar, and S. Levine, “Zero-shot robotic manipulation with pretrained image-editing diffusion models,” *arXiv preprint arXiv:2310.10639*, 2023.
- [25] G. Du, K. Wang, S. Lian, and K. Zhao, “Vision-based robotic grasping from object localization, object pose estimation to grasp estimation for parallel grippers: a review,” *Artificial Intelligence Review*, vol. 54, no. 3, pp. 1677–1734, 2021.
- [26] J. Yi, P. Liu, J. Gao, R. Yuan, and J. Wu, “An intelligent emulsion explosive grasping and filling system based on yolo-simam-grcnn,” *Scientific Reports*, vol. 14, no. 1, p. 28425, 2024.
- [27] B. Huang, J. Yu, and S. Jain, “Earl: Eye-on-hand reinforcement learner for dynamic grasping with active pose estimation,” in *2023 IEEE/RSJ International Conference on Intelligent Robots and Systems*. IEEE, 2023, pp. 2963–2970.
- [28] H. Tan, X. Xu, C. Ying, X. Mao, S. Liu, X. Zhang, H. Su, and J. Zhu, “Manibox: Enhancing spatial grasping generalization via scalable simulation data generation,” *arXiv preprint arXiv:2411.01850*, 2024.
- [29] M. Xu, Z. Xu, Y. Xu, C. Chi, G. Wetzstein, M. Veloso, and S. Song, “Flow as the cross-domain manipulation interface,” *arXiv preprint arXiv:2407.15208*, 2024.
- [30] M. Zawalski, W. Chen, K. Pertsch, O. Mees, C. Finn, and S. Levine, “Robotic control via embodied chain-of-thought reasoning,” *The Conference on Robot Learning 2024*, 2024.
- [31] N. Gkanatsios, A. Jain, Z. Xian, Y. Zhang, C. Atkeson, and K. Fragkiadaki, “Energy-based models are zero-shot planners for compositional scene rearrangement,” *Robotics Science and Systems*, 2023.
- [32] D. Park, Y. Seo, D. Shin, J. Choi, and S. Y. Chun, “A single multi-task deep neural network with post-processing for object detection with reasoning and robotic grasp detection,” in *2020 IEEE International Conference on Robotics and Automation (ICRA)*. IEEE, 2020, pp. 7300–7306.
- [33] H. Zhang, X. Lan, L. Wan, C. Yang, and N. Zheng, “A multi-task convolutional neural network for autonomous robotic grasping in object stacking scenes,” in *2019 IEEE/RSJ International Conference on Intelligent Robots and Systems*. IEEE, 2019, pp. 6435–6442.
- [34] J. Song, C. Meng, and S. Ermon, “Denoising diffusion implicit models,” *arXiv preprint arXiv:2010.02502*, 2020.
- [35] F. Lin, Y. Hu, P. Sheng, C. Wen, J. You, and Y. Gao, “Data scaling laws in imitation learning for robotic manipulation,” *arXiv preprint arXiv:2410.18647*, 2024.
- [36] A. Radford, J. W. Kim, C. Hallacy, A. Ramesh, G. Goh, S. Agarwal, G. Sastry, A. Askell, P. Mishkin, J. Clark, *et al.*, “Learning transferable visual models from natural language supervision,” in *International conference on machine learning*. PMLR, 2021, pp. 8748–8763.
- [37] A. Stone, T. Xiao, Y. Lu, K. Gopalakrishnan, K.-H. Lee, Q. Vuong, P. Wohlhart, S. Kirmani, B. Zitkovich, F. Xia, *et al.*, “Open-world object manipulation using pre-trained vision-language models,” *The Conference on Robot Learning 2023*, 2023.